Measurement of J/ψ production as a function of event activity in p+p collisions at $\sqrt{s}$ = 510 GeV with STAR at RHIC

Brennan Schaefer[1,*]

[1]Lehigh University, Bethlehem, Pennsylvania 18015

Abstract. We present dielectron channel measurements of J/ψ production at mid rapidity ($|y|$ <1) within $4 < p_T < 12$ GeV/c as a function of the mid-rapidity ($|\eta| < 1$) charged particle multiplicity. This study uses a larger data set than previous STAR measurements, enabling measurements over a wider multiplicity range with narrower bins. Consistent with measurements at 200 GeV [1], 7 TeV [2] and 13 TeV [3], a faster-than-linear rise in the self-normalized J/ψ yield is observed as a function of the charged-particle multiplicity. The divergence of the trends for RHIC and LHC at higher multiplicity values emphasizes the potential improvement that extending the measurement range may permit.

1 Introduction

In heavy ion collisions, a centrality dependent suppression of J/ψ production has been observed with increasing centrality coinciding with increasing suppression. Although such probes of the quark-gluon plasma are essential, the quarkonium production mechanism is not yet completely understood [4]. In order to provide a framework to approach this problem, measurements are needed of the dependence of quarkonium production on event multiplicity in p+p collisions.

NRQCD calculations [5, 6] featuring parton distribution functions of the colliding protons, a cross section for charm (anti)quark production, and a term for hadronization have been used to model the production. The widely varied length scales of these processes, from the inverse mass of the charm up to the size of the charmonium state, affords the factorization into these discrete terms. Using only hard scattering from the opposing partons, NRQCD under-predicts J/ψ production as a function of multiplicity and is qualitatively incongruent with the measured result [7].

Multi-parton interactions (MPI) [6] are additionally employed to better describe the faster-than-linear rise of charmonium production with respect to the event multiplicity. Events that feature more numerous interactions are more likely to feature small impact parameters of opposing partons, resulting in enhanced hard-scattering processes such as charmonium production [7]. Reciprocally, the percolation of color strings may cause a reduction of the soft hadron production and further contribute to the relative enhancement [8]. Extending the reach in multiplicity allows for the testing of the predictions made with these mechanisms.

*e-mail: brennan.schaefer@lehigh.edu

2 Experimental setup and dataset

The STAR detector is designed for a wide range of measurements. It is a nearly hermetic detector at RHIC with cylindrical geometry approximately 5.25 m in diameter and 6.2 m in length. The following STAR subsystems are used in this study. The Barrel Electromagnetic Calorimeter (BEMC) spans the pseudorapidity range $|\eta| < 1.0$ [9] with each tower covering approximately $\Delta\phi \times \Delta\eta = 0.05 \times 0.05$; the BEMC is used as a trigger detector and to measure the energies of $e^{\pm}$ candidates. The Time-of-Flight detector (TOF) [10] is a MRPC-based detector that sits at a radius of $r = 208$ cm from the beam line with a timing resolution of 100 ps; the TOF is used to reject associate tracks with speeds that are inconsistent with the $e^{\pm}$ hypothesis. The Vertex Position Detector (VPD) [11] covers the pseudorapidity range $4.24 < \eta < 5.1$ in both the forward and backward directions; it is used to trigger and to find the position of the collision vertex along the beam axis (z direction). The Beam-Beam Counter also sits at large rapidities and is used to trigger minimum-bias events [11]. The Time Projection Chamber (TPC) is used for tracking and to identify $e^{\pm}$ candidates based on measurements of their specific energy loss. The subsystems sit inside a 0.5 T solenoidal magnetic field. The dataset used in this analysis was recorded in the 2017 run period and consists of 79.5 pb^{-1} of p+p collisions at $\sqrt{s} = 510$ GeV, which is 4 times larger than the data set used to measure J/ψ production as a function of charged-particle multiplicity in p+p collisions at $\sqrt{s} = 200$ GeV [1].

3 Analysis Method

After triggering, events are selected based on the position of their primary collision vertex and other vertex quality selections. Candidate $e^{\pm}$ are selected based on their track quality, their specific energy energy loss in the TPC, and their energy deposition in the BEMC. Additional requirements are applied to the trigger and associate $e^{\pm}$ candidates in each pair. The trigger particle must be matched to the calorimeter hit that triggered the event. The energy-to-momentum ratio (E/pc) for the trigger particle must be within the expected limits for $e^{\pm}$, where the energy is measured in the calorimeter and the momentum is measured in the TPC. The associate track must either be matched to a hit in the TOF that passes a selection to exclude slow non-$e^{\pm}$, or it must be matched to a calorimeter hit that passes the selection on E/pc. The full list of specific track quality selections, along with the event-trigger and pair-associate selection parameters are listed in Tab. 1.

J/ψ candidates are reconstructed in the dielectron channel using the invariant mass method. The *unlike-sign* pair distribution is fit using a peak-plus-background function without prior subtraction of the *like-sign* distribution. This is necessary to minimize the associated statistical fluctuation and thus maximize the event multiplicity reach. In the fit, the peak is described with a CrystalBall function and the background is parameterized with a cubic polynomial. The centroid of the CrystalBall core is fixed to the PDG world average for the J/ψ mass [12]. A profile fit is made over the full multiplicity range, and this fit is used to set the CrystalBall variance parameter (σ) for subsequent fits in seven narrow multiplicity intervals. Three of the seven invariant mass plots are shown in Fig. 1. Yields are extracted from $2.6 < M_{ee} < 3.4$ GeV/c^2 and are corrected for areas outside this interval.

The Time-of-Flight detector sub-system has a timing resolution that is three orders of magnitude faster than the highest bunch-crossing rate at RHIC. The resulting imperviousness to out-of-bunch pile-up (for instance the effects of lingering space charges due to tracks from preceding bunch-crossing collisions) makes for an ideal quantity to characterize the multiplicity in each event. A less restrictive set of tracking quality requirements (compared to

Events	
$\lvert v_z \rvert$	< 40 cm

Track Quality	
p_T	> 0.2 GeV/c
η	–1.0 to 1.0
DCA	< 1.5 cm
$n_{\text{hits,fit}}$	≥ 20
$R_{\text{hits,fit}}$	> 0.52
$n_{\text{hits},dE/dx}$	≥ 11
$E_{\text{TOW}}/E_{\text{CLU}}$	> 0.5
$n\sigma_e$	–1.9 to 3.0

Trigger Electron	
E/pc	0.67 to 3.33
matched to BEMC HT trigger hit	

Associate Electron	
$1/\beta_{\text{TOF}}$	0.97 to 1.03
or	
E/pc	0.67 to 3.33

TOF Multiplicity	
$n_{\text{hits,fit}}$	≥ 15
DCA	1.5 cm
η	–1.0 to 1.0
p_T	> 0.2 GeV/c
matched to TOF hit	

Table 1: Event and track selection requirements. Here, v_z is the z coordinate of the primary collision vertex, measured with respect to the nominal center of the STAR detector and with the z axis coinciding with the beam direction. *DCA* is the distance of closest approach of the helical track to the primary vertex. The quantity $n_{\text{hits,fit}}$ is the number of measured space points along the particle trajectory. $R_{\text{hits,fit}}$ is the ratio of that number to the maximum possible number of space points. The quantity $n_{\text{hits},dE/dx}$ is the number of space points that are used to determine the specific energy loss. The quantity $n\sigma_e$ is the difference between the specific energy loss measured in the TPC and the expected value for $e^{\pm}$, divided by the dE/dx resolution of the TPC. The particle speed measured in the TOF is denoted β_{TOF}.

those required to select electrons and positrons) is additionally applied to each track counted in the multiplicity, and may be found in Tab. 1.

The matching of inner tracks to outer TOF hit positions is done by projecting their helical trajectories and limiting the difference to the measured outer hit position [13]. The resulting TOF-counted event multiplicity (*TOFmult* hereafter) is anti-correlated with the rate of minimum-bias collisions (having a hit in both sides of the BBC) as shown in Fig. 2. The decreasing *TOFmult* is understood to be the result of obscuring of tracks within the higher density of concurrent TPC tracks. Following a quadratic fit, a luminosity flattening procedure adjusts the average *TOFmult* to the projected fit maximum. The flattening is performed independently for the minimum-bias and high-tower triggered datasets.

While the luminosity flattening procedure adjusts the numbers of tracks per event, an efficiency study is needed to correct the number of events for given charged particle multiplicity bias due in the event reconstruction. To this end, PYTHIA8 simulated events are embedded into zerobias events and fully reconstructed. The vertex-finding efficiency, the efficiency associated with the vertex quality or colloquially the *ranking* selection, as well as the forward detector hit requirement for high-tower (VPD) and minimum-bias (BBC) events are studied by comparing the number of events simulated versus those that pass the selections. The yields used in calculating the self-normalized yields (Sec. 5) are corrected using the results shown in Fig. 3.

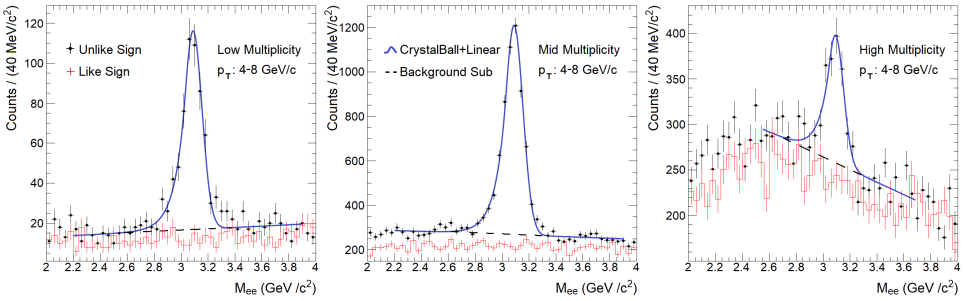

Figure 1: Examples of fitted invariant mass plots are shown for the lowest, middle, and highest of the charged particle multiplicity intervals.

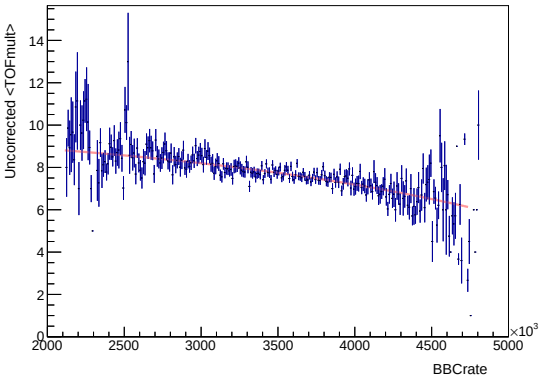

Figure 2: The as-measured *TOFmult* versus BBCrate is fitted with a quadratic that is subsequently used to flatten the distribution. This accounts for the diminished efficiency with increasing luminosity.

4 Uncertainties

The statistical uncertainty in the self-normalized J/ψ yields ranges from 3–26%. Eight sources are included in the estimate of the systematic uncertainty. The track-quality selections, E/pc, BEMC trigger, and β_{TOF} selections are varied. Alternate methods are used to extract the J/ψ yield from the histogram and fit. Alternate functional forms are used for the correction of *TOFmult* as a function of the luminosity. The results are summarized in Table 2. The total systematic uncertainty ranges from 3–17%.

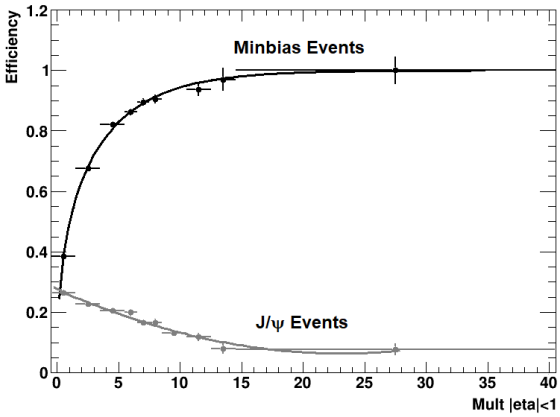

Figure 3: Separate efficiency versus charged particle multiplicity event selection corrections are necessary for the J/ψ and minimum-bias distributions.

Systematic Uncertainties	%
Track Quality	1 - 12
Daughter Electron Selection	1 - 9
Trigger Efficiency Correction	0 - 13
Signal & Background Distinction	3 - 16
Total	3 - 17

Table 2: Ranges of systematic uncertainty categories.

5 Results and conclusions

Figure 4 shows the self-normalized J/ψ yield as a function of the self-normalized event multiplicity for different multiplicity intervals. Notwithstanding the large uncertainties, the highest point can be interpreted as indicating that J/ψ production rates are thirty times higher than average in the event class having 5 times the average charged-particle multiplicity.

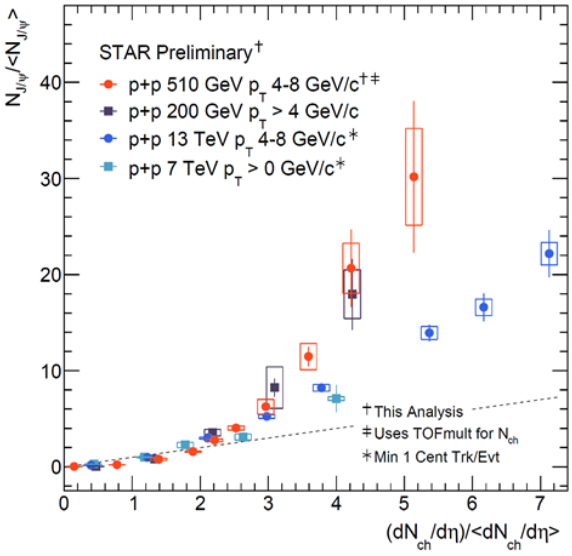

Figure 4: The self-normalized J/ψ yields versus normalized charged particle multiplicity are shown at four collision energies [1–3].

The resulting yields feature a faster-than-linear rise in production with respect to charged particle multiplicity for RHIC [1] and LHC [2, 3] collision energies. The results shown first in this work (red circle markers) are consistent with the results at $\sqrt{s}$ = 200 GeV while benefiting from improved granularity in multiplicity. The $\sqrt{s}$ = 200 GeV, 510 GeV and 13 TeV results are measured with comparable J/ψ transverse momentum ranges. It should be noted that the RHIC and LHC results all determine multiplicity classes based on the mid-rapidity ($|\eta| < 1$) charged-particle multiplicity. The results are tentatively indicative of different J/ψ production trends as a function of multiplicity for RHIC and LHC collision energies. This difference is seen in PYTHIA, but further theoretical studies may be needed to fully explain it. Further STAR measurements using larger data sets or calculating the charged-particle multiplicity in other pseudorapidity ranges may also help shed light on the evolution of J/ψ production as a function of event activity.

References

[1] J. Adam et al. (STAR), J/ψ production cross section and its dependence on charged-particle multiplicity in p+p collisions at $\sqrt{s}$=200 GeV, Physics Letters B **786**, 87 (2018). https://doi.org/10.1016/j.physletb.2018.09.029

[2] J. Adam et al. (ALICE), Measurement of charm and beauty production at central rapidity versus charged-particle multiplicity in proton-proton collisions at $\sqrt{s}$ = 7 TeV, JHEP **09**, 148 (2015), 39 pages, 11 captioned figures, 2 (+6) tables, authors from page 34, published version, figures at http://aliceinfo.cern.ch/ArtSubmission/node/1599, 1505.00664. 10.1007/JHEP09(2015)148

[3] S. Acharya et al. (ALICE), Multiplicity dependence of inclusive J/ψ production at midrapidity in pp collisions at $\sqrt{s}$ = 13 TeV, Physics Letters B **810**, 135758 (2020). https://doi.org/10.1016/j.physletb.2020.135758

[4] J. Adam et al. (STAR Collaboration), Measurements of the transverse-momentum-dependent cross sections of J/ψ production at mid-rapidity in proton + proton collisions at $\sqrt{s}$ = 510 and 500 GeV with the STAR detector, Phys. Rev. D **100**, 052009 (2019). 10.1103/PhysRevD.100.052009

[5] Y.Q. Ma, R. Venugopalan, Comprehensive description of J/ψ production in proton-proton collisions at collider energies, Phys. Rev. Lett. **113**, 192301 (2014), 1408.4075. 10.1103/PhysRevLett.113.192301

[6] S.G. Weber, A. Dubla, A. Andronic, A. Morsch, Elucidating the multiplicity dependence of J/ψ production in proton–proton collisions with PYTHIA8, The European Physical Journal C **79** (2019). 10.1140/epjc/s10052-018-6531-4

[7] B. Abelev et al., J/ψ production as a function of charged particle multiplicity in pp collisions at $\sqrt{s}$=7 TeV, Physics Letters B **712**, 165–175 (2012). 10.1016/j.physletb.2012.04.052

[8] E.G. Ferreiro, C. Pajares, High multiplicity pp events and J/ψ production at energies available at the CERN Large Hadron Collider, Phys. Rev. C **86**, 034903 (2012). 10.1103/PhysRevC.86.034903

[9] M. Beddo et al., The STAR barrel electromagnetic calorimeter, Nuclear Instruments and Methods in Physics Research Section A: Accelerators, Spectrometers, Detectors and Associated Equipment **499**, 725 (2003), the Relativistic Heavy Ion Collider Project: RHIC and its Detectors. https://doi.org/10.1016/S0168-9002(02)01970-8

[10] M. Shao, O. Barannikova, X. Dong, Y. Fisyak, L. Ruan, P. Sorensen, Z. Xu, Extensive particle identification with TPC and TOF at the STAR experiment, Nuclear Instruments and Methods in Physics Research Section A: Accelerators, Spectrometers, Detectors and Associated Equipment **558**, 419 (2006). https://doi.org/10.1016/j.nima.2005.11.251

[11] W. Llope et al., The STAR Vertex Position Detector, Nuclear Instruments and Methods in Physics Research Section A: Accelerators, Spectrometers, Detectors and Associated Equipment **759**, 23 (2014). https://doi.org/10.1016/j.nima.2014.04.080

[12] M. Tanabashi, et al., J/ψ(1S) mass, Phys.Rev.D 030001 **98** (2018). https://pdg.lbl.gov/2018/listings/rpp2018-list-J-psi-1S.pdf

[13] M. Anderson et al., The STAR Time Projection Chamber: a unique tool for studying high multiplicity events at RHIC, Nuclear Instruments and Methods in Physics Research Section A: Accelerators, Spectrometers, Detectors and Associated Equipment **499**, 659–678 (2003). 10.1016/s0168-9002(02)01964-2